A Search for Warm Circumstellar Disks in the TW Hydrae Association

(Accepted for Publication in Astronomical Journal, April 2004 issue)

A. J. Weinberger

Department of Terrestrial Magnetism, Carnegie Institution of Washington,
and NASA Astrobiology Institute
5241 Broad Branch Road, NW, Washington, DC 20015

weinberger@dtm.ciw.edu

E. E. Becklin, B. Zuckerman, and I. Song.

Division of Astronomy, University of California Los Angeles
and NASA Astrobiology Institute
Box 951562, Los Angeles, CA 90095-1562

becklin,ben,song@astro.ucla.edu

ABSTRACT

A search for previously undetected optically thin disks around stars in the nearby, young, TW Hydrae Association was conducted around sixteen stars with sensitive 12 and 18 μm photometry. The survey could detect Zodiacal-like dust, with temperature 200–300 K, at levels of $L_{IR}/L_{\star}$=7×10^{-3}. Possible mid-infrared excess emission from TWA 17 was detected at the 2σ level, but none of the other stars showed evidence for circumstellar dust. The rapid disappearance of large amounts of dust around the K and M-type stars in this sample may mean that any planet formation in the terrestrial planet region was completed very quickly. There appears to be a bi-modal distribution of dust disks in TWA with stars having either copious or negligible warm dust.

Subject headings: stars: pre–main-sequence — stars: late type — circumstellar matter — planetary systems: protoplanetary disks

1. Introduction

The TW Hydrae Association (TWA) provides an excellent laboratory in which to study the evolution of dusty disks. This collection of 24 star systems within $\sim$40 pc of each other (de la Reza et al. 1989; Webb et al. 1999; Sterzik et al. 1999; Webb 2000; Zuckerman et al. 2001; Song, Zuckerman, & Bessell 2003) is one of the the closest ($\sim$60 pc) young stellar groups to Earth. Primary members range in spectral type from A0 to M3 and have common ages of 5–10 Myr as determined from pre-main sequence tracks, Li abundances and X-ray fluxes. Thus TWA stars are poised between T Tauri and main sequence stages of stellar evolution.

Inner (radius $<$ 0.1 AU) disks around weak-lined T Tauri stars are observed to dissipate very quickly, in $\lesssim$6 Myr, and contemporaneously with the cessation of accretion (Haisch, Lada, & Lada 2001). For planet formation, it is of interest how quickly material dissipates further out in the disk, so observations at longer wavelengths sensitive to colder dust are necessary. Results from ISO (Spangler et al. 2001; Meyer & Beckwith 2000) again suggest that disks at 0.3-20 AU disappear quickly.

Dusty disks around four TWA stars were inferred from excess infrared emission discovered with the Infrared Astronomical Satellite (IRAS), and they are strikingly diverse. The A0 star HR 4796A (TWA 11) has a narrow ring of dust located at 70 AU (Jayawardhana et al. 1998; Koerner et al. 1998; Schneider et al. 1999; Telesco et al. 2000). TW Hya (TWA 1) has a broad face-on disk that extends more than 135 AU from the star with a dip in surface brightness at ∼110 AU (Krist et al. 2000; Wilner et al. 2000; Weinberger et al. 2002). TW Hya's disk still contains much molecular gas (Kastner et al. 1997) while HR 4796A's has no detectable gas (Greaves, Mannings, & Holland 2000). IRAS also measured excess emission from Hen 3-600 and HD 98800, which are both multiple stars where the dust responsible for the infrared excess encircles one member (Jayawardhana et al. 1999a; Gehrz et al. 1999) while cooler dust detected at submillimeter wavelengths may be in circumbinary orbits (Zuckerman 2001). The amount of dust, characterized by the fraction of the star's luminosity which is re-radiated in the mid-to-far-infrared (f), is 5×10^{-3} for HR 4796A and much larger for the other three stars (f=0.1–0.3; Zuckerman, Forveille, & Kastner (1995)).

The IRAS Faint Source Catalog, complete (SNR≈5) to a flux density limit of ∼0.2 Jy at 12 and 25 μm, had insufficient sensitivity to probe fully for disks in TWA. At the distance to and age of TWA, 12 μm stellar photospheric emission was detectable by IRAS only for spectral types earlier than K0. We have performed a ground based search with better sensitivity to search for warm circumstellar disks that might lurk around sixteen TWA stars.

2. Observations, Data Analysis, and Photometry

Observations were made at the W. M. Keck Observatory using the facility instrument Long Wavelength Spectrometer (LWS) (Jones & Puetter 1993). LWS uses a 128×128 pixel Boeing Si:As detector, and has a plate scale of 0.080 arcsec pixel^{-1}, resulting in a focal-plane field of view of $10.2''$ square. The characteristics of the filters used in this project are given in Table 1. L′ band (3.8 μm) measurements were obtained for two purposes: (1) quickly locating the star on the array and (2) providing a long wavelength point for calculations of stellar photospheric fluxes. We used the most sensitive 12 and 18 μm filters available during each run; the SiC and 17.65 filters were added in 2001 and so were not available at the start of this project. TWA 5–25 are all identified as members of TWA in Webb et al. (1999), Sterzik et al. (1999), Zuckerman et al. (2001), or Song, Zuckerman, & Bessell (2003).

A summary of the photometric properties of the six nights used for observations is given in Table 2. All six nights were clear of clouds. During each night, infrared standard stars were observed approximately every two hours and a photometric calibration for each night of observations was obtained using all standards from that night. Sensitivities were characterized in terms of an instrumental magnitude (mag $-2.5\log(\mathrm{adu/s})$) and are given in Table 2. These standards were usually at small airmass (1–1.6) compared to the TWA targets, but on two nights – 6 Feb 2001 and 29 May 2003, standards were observed at airmasses up to 3.3 and used to determine airmass corrections in units of mag airmass^{-1}. Standard deviations of measurements of multiple standards and linear fits to the sensitivity as a function of airmass were used to determine the calibration uncertainty. This was taken to be the systematic error in the photometry of the target stars.

We employed a standard chop-nod scheme for background removal, in which the target star image falls on the detector in either two or all four observed positions. The telescope's secondary mirror was chopped 5–10″ north-south at frequencies of ∼5 Hz, and images from each chop position were summed. After ∼30 s, the telescope was nodded the same distance as the chop and images were again summed in both chop positions. The double difference $((nod_1chop_1 - nod_1chop_2) - (nod_2chop_1 - nod_2chop_2))$ was used to remove the thermal

background from the sky and telescope. Total on-star integration times are given in Tables 3–5.

Different LWS filters place images at different locations on the detector, so standard stars were used to determine the shifts between the L′, 12, and 18 μm filters. For filters in which the targets were not visible at high SNR, the predetermined shifts were used to locate the target. The uncertainty in the prediction is about one pixel, probably due to offset guiding errors.

The seeing at airmass 1.5 was 0.8″ at L′-band and 0.5″at 12 and 18 μm for 2000 and 2001 runs and 0.5″at L′-band and 0.4″ at 12 and 18 μm during the 2002 run. The image size at higher airmass was measured on 6 Feb 2001 and 29 May 2002 and was consistent with seeing proportional to $(\cos z)^{0.6}$.

The flux density of each star was measured with synthetic aperture photometry on the double differenced images in a beam of radius 14 pixels ($\sim$1″). These measurements were corrected to the total flux by measuring an aperture correction from the standard stars. Imperfect background subtraction was accounted for by subtracting a "sky" value measured in an annulus around the star. Although, in principle, higher SNR photometry is obtained with an aperture radius approximately equal to the FWHM of the stars, we used a larger beam so we would be insensitive to the uncertainty in the location of the object in the filters where it was not seen at high SNR. The photometric uncertainties reported are a combination of the sky noise, the Poisson noise from the stellar measurement, and the systematic calibration uncertainty described above. We estimate at most an additional 2% uncertainty from pixel-pixel sensitivity variations across the array; the images were not flat-fielded.

3. Results

Photometric measurements of the sixteen target stars are given in Tables 3-5. All but three were detected at 12 μm with SNR$>$3. None of the stars was detected with SNR$>$3 at 18 μm.

3.1. Assessing the Presence of Infrared Excess

We fit stellar photosphere models (Hauschildt et al. 1999) to J, H, and Ks-band data from the 2MASS catalog and our L′-band data where available. We treated the stellar effective temperature and the model normalization as unknowns and performed a chi-squared minimization to determine these parameters. The models have temperature bins of 100 K in the region 1700–4000 K and 200 K in the region 4000–10000 K. The best fit models were used to predict the photospheric flux densities at 12 and 18 μm that are reported in Tables 4 and 5.

It is not obvious how to assess the uncertainties in the photospheric model predictions other than by comparison with measurements of stars without excess. As a test, instead of using the best fit temperatures, we used the Hartigan, Strom, & Strom (1994) and Luhman & Rieke (1998) temperature scales for dwarfs to convert published spectral types to effective temperatures and compared the resulting predictions. On average, the predictions were the same, i.e. there was no bias. The scatter in the difference of the predictions was 15%. We take this to be an upper limit on the uncertainty in our knowledge of the photospheres because it could be affected by incorrect spectral typing.

At 12 and 18 μm, all of our measurements agree to within 3 σ with the model predictions. In one object, TWA 17, both the 12 and 18 μm flux densities exceed the photospheric predictions, as seen in Figure 1. Using the total uncertainties on both points, its excess is significant only at 2.2σ. The color temperature of this excess is 170 K and corresponds to 0.005 L_*. Three of the stars in our sample were previously observed by Jayawardhana

et al. (1999b) – TWA 5A, TWA 6, and TWA 7. The results for TWA 6 and 7 agree within 1σ. However, the measurement reported here for TWA 5A at 12 μm, 63.4 $\pm$ 7.4 mJy differs by 4σ from their N-band (8–13 μm) measurement of 96 $\pm$ 9 mJy. Therefore, we do not confirm the excess they suggested around TWA 5A.

To quantify the limits on the amount of excess emission that could be present around each star, we found the maximum luminosity blackbodies consistent with the 3 σ upper limits of the measured 12 and 18 μm flux densities. Real disks are likely to have dust at a range of temperatures, and we do not know the disk energy distributions a priori. So we take the simplest case of blackbodies at three temperatures – 100, 200, and 300K. We characterize the upper limit on the excess at each of these temperatures by $L_{BB}/L_\star$ and report these values in Table 6. A sample set of fits is shown in Figure 2 for TWA 12. Given our sensitivities at 12 and 18 μm, we are most sensitive to dust at 200-300K. For comparison, HR 4796 has $L_{IR}/L_\star$=5$\times10^{-3}$ at T=110 K (Jura et al. 1993), although for this A-type star its dust is at Kuiper-belt like distances. For 300 K dust, in the terrestrial planet region around the sample stars, we could detect $L_{IR}/L_\star$=5$\times10^{-3}$ for 9 of the 16 TWA stars.

4. Discussion

Most previous surveys of post T-Tauri star dust have concentrated on $\sim$1000 K dust, observable at L-band. This dust resides at tens of stellar radii only. One set of surveys show that these inner edges disappear at 3–6 Myr, shortly after accretion ends (Haisch, Lada, & Lada 2001). A survey of the mostly very low mass members of the η Cha cluster, however, finds a high hot disk fraction even at an age of 5–8 Myr (Lyo et al. 2003). Whether these differences stem from sample selection effects, birth conditions or some other variables remains to be determined.

Our measurements constrain the amount of dust at temperatures of $\sim$200 K. For the TWA stars, this corresponds to distances of 1–5 AU, depending on the luminosity of the star and the emissivity of the grains. The median spectral type of our sample is M0 with a luminosity of $\sim$0.25 $L_\odot$. Grains that absorb and emit like blackbodies reach a temperature of 200 K at 1 AU for such a star while interstellar silicates at 200 K are at 4 AU.

Converting the infrared excess limits to dust masses is hampered by our lack of knowledge of the dust grain size distribution. For example, if all the grains in a disk had radius 20 μm, approximately the size our observations are most sensitive to, had a semi-major axis of 1 AU, and total $L_{IR}/L_\star$= 0.01, their mass would be $\sim10^{-5}$ M_{Earth}. However, if the number of grains of a given radius followed a power-law distribution with slope -3.5 and a maximum size of 1000 km, the dust mass would be 5 orders of magnitude larger.

Dust around young stars could come in two forms: primordial material, largely unprocessed from the interstellar medium, or debris generated in collisions of planetesimals. The material around at least one member of TWA, HR 4796A, is likely debris (Jura et al. 1995; Schneider et al. 1999) based on its inferred size, color, and albedo. So, planetesimals evidently have had time to form around this A0 star. The dust around TW Hya itself, a K7 star, is likely a mixture of primordial and debris based on the grain size distribution which is larger than interstellar (Weinberger et al. 2002).

Primordial, i.e. interstellar, dust distributions, are dominated by small ($\lesssim$1 μm) grains. Our observations would be very sensitive to primordial dust, and therefore it is likely that the stars for which we obtain upper limits on excesses have already lost such material.

Models of planetesimal formation produce copious quantities of dust during an epoch where large bodies perturb each other and generate many collisions (e.g. Kenyon & Bromley 2002). In our own Solar System, collisions must have occurred in the terrestrial planet region, at least at a low level, for 30 Myr, the likely time of the Moon forming impact (Yin et al. 2002).

Given the low dust limits set by our observations of TWA members, the era of frequent collisions must have stopped at 1–4 AU long enough ago for little dust to remain at temperatures of $\sim$200 K. In models of terrestrial accumulation, dust formation declines exponentially over 1–2 Myr after peaking during the formation of 1000-2000 km bodies (Kenyon & Bromley 2004). By 3 Myr after this period, they predict an $L_{IR}/L_{\star}$ of $<$1e-3. Roughly then, the epoch of large planetesimal growth must have ended about 1 Myr ago for the dust to have disappeared. Thus, the absence of material in the terrestrial planet region implied by the non-detections of our survey may mean that planet formation has already taken place. Some evidence for rapid planet formation may in fact exist in the structure of the debris around HR 4796A which is confined to a very narrow ring with brightness asymmetry (Schneider et al. 2003).

It appears from radial velocity surveys that giant planets commonly orbit main sequence Solar type stars, but less frequently orbit the M-type stars that comprise most of our sample (Gould, Ford, & Fischer 2003). Only one star in the TW Hydrae association, TW Hya itself, is a single star with large amounts of dust and gas remaining. Given the current statistics, it is possible that planets do form only in the long lived disks like that surrounding TW Hya. However, the number of known planets is likely to grow as lower masses and longer orbits are probed by experiments, and this study shows that there are no other long lived disks in the TW Hya association that can still form planets.

5. Conclusions

This survey could detect small amounts of dust, similar to that found around the well studied TW Hya Association A-type star HR 4796A, around the late-type members of the association. No new stars with infrared excess at 12 or 18 μm were positively discovered in this most sensitive survey to date. It is remarkable that of the 24 star systems now known in the TW Hydrae association, all of those with dust were discovered by IRAS despite the ten times better sensitivity of this survey. Dust content in TWA is bimodal, with a few stars possessing much dust and most largely devoid of material. In regions analogous to the terrestrial planet region, even at the young age of 5–10 Myr, little material remains or is being generated in collisions around these late-type stars.

This paper is based on observations at the W. M. Keck Observatory, which is operated as a scientific partnership between the California Institute of Technology, the University of California, and NASA, and was made possible by the generous financial support of the W. M. Keck Foundation. We recognize the importance of Mauna Kea to Hawaiians. We received valuable assistance with observations from Randy Campbell, Meg Whittle, Joel Aycock, and Ron Quick. We acknowledge support from NASA Origins of Solar Systems grants to UCLA and CIW. This publication makes use of data products from the Two Micron All Sky Survey funded by NASA and NSF. We thank Anna Haugsjaa, an NSF Research Experience for Undergraduates summer intern at CIW for her work on this project.

REFERENCES

de la Reza, R., Torres, C.A.O., Quast, G., Castilho, B.V., & Vieira, G.L. 1989, ApJ, 343, 61

Gehrz, R. D., Smith, N., Low, F. J., Krautter, J., Nollenberg, J. G., & Jones, T. J. 1999, ApJ, 512, L55

Gould, A., Ford, E. B., & Fischer, D. A. 2003, ApJ, 591, L155

Greaves, J. S., Mannings, V., & Holland, W. S. 2000, Icarus, 143, 155

Haisch, K. E., Lada, E. A., & Lada, C. J. 2001, ApJ, 553, L153

Hartigan, P., Strom, K. M., & Strom, S. E. 1994, ApJ, 427, 961

Hauschildt, P. H., Allard, F., Ferguson, J., Baron, E., & Alexander, D. R. 1999, ApJ, 525, 871

Jayawardhana, R., Fisher, S., Hartmann, L., Telesco, C., Pina, R. & Fazio, G. 1998, ApJ, 503, L79

Jayawardhana, R., Hartmann, L., Fazio, G., Fisher, R. S., Telesco, C. M., & Piña, R. K. 1999a, ApJ, 520, L41

Jayawardhana, R., Hartmann, L., Fazio, G., Fisher, R. S., Telesco, C. M., & Piña, R. K. 1999b, ApJ, 521, L129

Jones, B., & Puetter, R. 1993, in Proc. SPIE vol. 1946, 610

Jura, M., Zuckerman, B., Becklin, E.E. & Smith, R.C. 1993, ApJ, 418, L37

Jura, M., Ghez, A. M., White, R. J., McCarthy, D. W., Smith, R. C., & Martin, P. G. 1995, ApJ, 445, 451

Kastner, J. H., Zuckerman, B., Weintraub, D. A., & Forveille, T. 1997, Science, 277, 67

Kenyon, S. J. & Bromley, B. C. 2002, ApJ, 577, L35

Kenyon, S. J. & Bromley, B. C. 2004, ApJ, submitted

Koerner, D. W., Ressler, M. E., Werner, M. W. & Backman, D. E. 1998, ApJ, 503, L83

Krist, J. E., Stapelfeldt, K. R., Ménard, F. Padgett, D. L. & Burrows, C. J. 2000, ApJ, 538, 793

Low, F. J., Hines, D. C., & Schneider, G. 1999, ApJ, 520, L45

Lowrance, P. J. et al. 1999, ApJ, 512, L69

Luhman, K. L. & Rieke, G. H. 1998, ApJ, 497, 354

Lyo, A.-R., Lawson, W. A., Mamajek, E. E., Feigelson, E. D., Sung, E., & Crause, L. A. 2003, MNRAS, 338, 616

Meyer, M. R. & Beckwith, S. V. W. 2000, ISO Survey of a Dusty Universe, Proceedings of a Ringberg Workshop Held at Ringberg Castle, Tegernsee, Germany, 8-12 November 1999, Edited by D. Lemke, M. Stickel, and K. Wilke, Lecture Notes in Physics, vol. 548, p.341, 341

Schneider, G. et al. 1999, ApJ, 513, L127

Schneider, G., Weinberger, A.J., Smith, B.A., Becklin, E.E., Silverstone, M.J., Hines, D.C. & Lowrance, P.J. 2003, in preparation for AJ

Song, I., Zuckerman, B., & Bessell, M. S. 2003, ApJ, 599, in press (Dec 10 issue)

Spangler, C., Sargent, A. I., Silverstone, M. D., Becklin, E. E., & Zuckerman, B. 2001, ApJ, 555, 932

Sterzik, M. F., Alcala, J. M., Covino, E., & Petr, M. G. 1999, A&A, 346, L41

Telesco, C. M. et al. 2000, ApJ, 530, 329

Webb, R. A., Zuckerman, B., Platais, I., Patience, J., White, R. J., Schwartz, M. J., & McCarthy, C. 1999, ApJ, 512, L63

Webb, R. A. 2000, PhD Thesis (UCLA)

Weinberger, A. J., Becklin, E. E., Schneider, G., Chiang, E. I., Lowrance, P. J., Silverstone, M., Zuckerman, B., Hines, D. C., & Smith, B. A. 2002, ApJ, 566, 409

Wilner, D. J., Ho, P. T. P., Kastner, J. H. & Rodríguez, L . F. 2000, ApJ, 534, L101

Yin, Q., Jacobsen, S. B., Yamashita, K., Blichert-Toft, J., Telouk, P., & Albarede, F. 2002, Nature, 418, 949

Zuckerman, B. Forveille, T., & Kastner, J. H. 1995, Nature, 373, 494

Zuckerman, B. 2001, ARA&A, 39, 549

Zuckerman, B., Webb, R. A., Schwartz, M., & Becklin, E. E. 2001, ApJ, 549, L233

This preprint was prepared with the AAS LaTeX macros v5.2.

Table 1. Filter parameters

Name	Central Wavelength (μm)	Bandpass (μm)	Zero mag Flux Density (Jy)
L′	3.85	3.5–4.2	251.0
11.7	11.67	11.2–12.2	29.9
SiC	11.77	10.5–12.9	29.6
17.65	17.74	17.3–18.2	12.9
17.9	17.9	16.9–18.9	12.7

Table 2. Nightly Photometric Sensitivities

Date of Observation	L′ Zero point	L′ air mass correction	N-band Zero point	N air mass correction	Q-band Zero point	Q air mass correction	Stars observed
2000 Dec 11	···	···	13.56 ± 0.07	0.27	11.33 ± 0.04	0.31	TWA 6
2001 Feb 05	···	···	13.46 ± 0.09	···	11.03 ± 0.11	0.29	TWA 7, 16
2001 Feb 06	15.34	0.03	13.49 ± 0.09	0.09	11.31 ± 0.09	0.39	TWA 5, 12, 13, 15, 17
2002 May 28	···	···	14.70	···	11.38	···	TWA 14, 18, 25
2002 May 29	15.79	···	14.71 ± 0.04	0.18	11.25 ± 0.18	0.54	TWA 19
2002 Jun 01	15.74	···	14.69	···	11.29	···	TWA 23

Note. — Zero points are given as instrumental magnitudes and airmass corrections are given as magnitudes per unit airmass. The N and Q-band values listed correspond to the SiC and 17.65 filters on 2002 May 28 and Jun 01 and for the 11.7 and 17.9 μm filters otherwise.

Table 3. Target Star Properties and L′-band Results

Star	Sp. Type	Airmass	time (s)	Flux Density (mJy)	Statistical Unc. (mJy)	Total Unc. (mJy)
TWA 5	M1.5	1.75	48	555.7	4.4	28.4
TWA 6	K7	1.73	30	217.2	5.8	12.4
TWA 12	M2	2.30	192	154.5	2.1	57
TWA 13N	M2	1.72	96	262.3	3.0	9.3
TWA 13S	M1	1.72	96	270.2	3.4	14.0
TWA 14	M0	2.46	45	118.9	4.1	8.4
TWA 15A	M1.5	2.68	96	35.4	3.1	3.9
TWA 15B	M2	2.68	96	38.0	3.1	4.0
TWA 17	K5	2.45	96	76.8	3.2	5.7
TWA 18	M0.5	2.29	30	80.9	4.7	6.6
TWA 19A	G5	2.86	30	230.1	4.9	16.6
TWA 19B	K7	2.89	30	124.0	4.9	9.9
TWA 23	M1	1.66	30	238.9	5.2	12.9
TWA 25	M0	2.00	60	327.7	4.8	18.2

Table 4. 12 μm Results

Star	Airmass	filter	time (s)	Flux Density (mJy)	Statistical Unc. (mJy)	Total Unc. (mJy)	Prediction (mJy)
TWA 5	1.86	11.7	192	63.4	4.5	7.4	63.1
TWA 6	1.64	11.7	120	20.3	5.5	5.5	29.5
TWA 7	1.91	11.7	120	70.4	5.6	8.6	76.4
TWA 12	2.56	11.7	384	16.7	3.0	3.5	17.5
TWA 13N	1.72	11.7	192	36.5	4.7	5.7	29.8
TWA 13S	1.72	11.7	192	36.0	4.3	5.4	30.7
TWA 14	2.59	SiC	216	12.4	3.8	3.8	13.5
TWA 15A	2.67	11.7	240	4.2	5.1	5.1	4.0
TWA 15B	2.67	11.7	240	-1.7	5.2	5.2	4.3
TWA 16	2.40	11.7	192	22.1	4.6	5.2	27.7
TWA 17	2.45	11.7	192	15.5	4.8	5.1	8.7
TWA 18	2.29	SiC	216	10.8	3.5	3.5	9.2
TWA 19	2.87	11.7	120	18.6	3.9	3.9	26.1
TWA 19B	2.90	11.7	216	11.1	2.7	2.7	14.1
TWA 23	1.67	SiC	216	27.4	2.9	3.1	27.1
TWA 25	2.01	SiC	216	41.9	4.2	4.5	37.2

Table 5. 18 μm Results

Star	Airmass	filter	time (s)	Flux Density (mJy)	Statistical Unc. (mJy)	Total Unc. (mJy)	Prediction (mJy)
TWA 5	1.83	17.9	618	27.4	16.4	16.6	16.6
TWA 6	1.71	17.9	983	7.1	12.6	12.6	12.6
TWA 7	1.95	17.9	319	-10.9	31.5	31.6	31.6
TWA 12	2.24	17.9	618	17.2	20.8	20.9	20.9
TWA 13N	1.73	17.9	618	-0.3	17.1	17.1	17.1
TWA 13S	1.73	17.9	618	11.8	18.5	18.5	18.5
TWA 14	2.48	17.65	408	29.7	38.6	39.1	39.1
TWA 15A	2.67	17.9	618	-16.3	25.4	25.5	25.5
TWA 15B	2.67	17.9	618	21.6	24.7	24.8	24.8
TWA 16	2.42	17.9	319	41.7	40.3	41.1	41.1
TWA 17	2.44	17.9	618	30.8	22.3	22.5	22.5
TWA 18	2.31	17.65	408	46.8	32.2	33.5	33.5
TWA 23	1.69	17.65	408	22.3	25.6	25.9	25.9
TWA 25	2.03	17.65	408	-19.3	29.9	30.1	30.1

Table 6. 3σ $L_{IR}/L_{\star}$ ($\times 10^{-3}$) limits for disk detection at three dust temperatures

Star	100 K	200 K	300 K
TWA 5	4.0	1.1	1.0
TWA 6	8.3	3.0	3.1
TWA 7	6.4	1.8	1.7
TWA 12	15.8	3.6	3.0
TWA 13N	6.8	2.5	2.7
TWA 13S	7.4	2.5	2.6
TWA 14	50.9	10.9	8.6
TWA 15A	98.7	24.0	20.5
TWA 15B	85.8	21.1	18.1
TWA 16	44.0	9.8	7.8
TWA 17	50.1	14.2	13.3
TWA 18	88.6	19.1	15.1
TWA 19A	15.8	2.4	1.4
TWA 19B	41.4	8.5	6.3
TWA 23	14.4	3.3	2.8
TWA 25	10.6	2.3	1.9

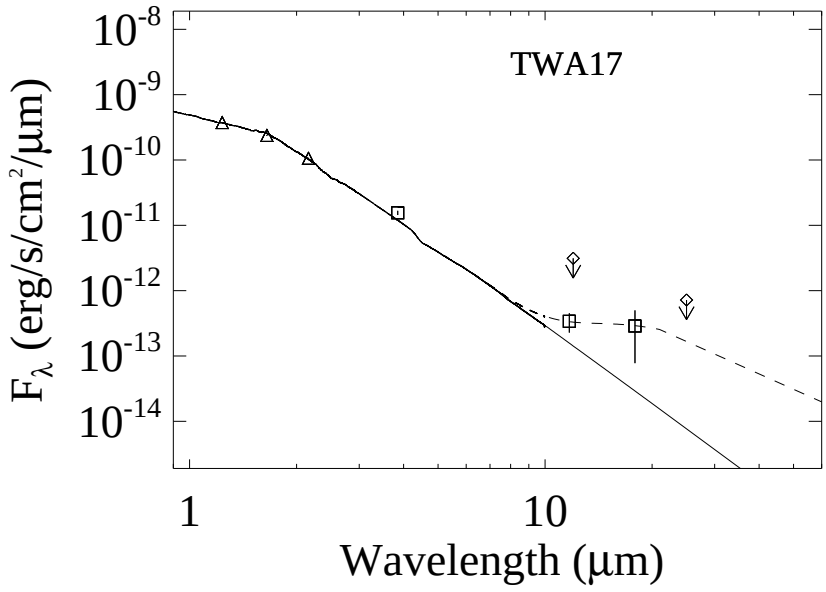

Fig. 1.— Spectral energy distribution of TWA 17. Triangles are J, H, and Ks data from 2MASS, squares are the LWS data reported in this paper, diamonds are the 150 mJy completeness level of IRAS at 12 μm and extrapolated to 18μm. The dotted line shows a 170 K blackbody, the best fit (i.e. color temperature) of the possible excess we measure, corresponding to $L_{IR}/L_\star$= 0.005.

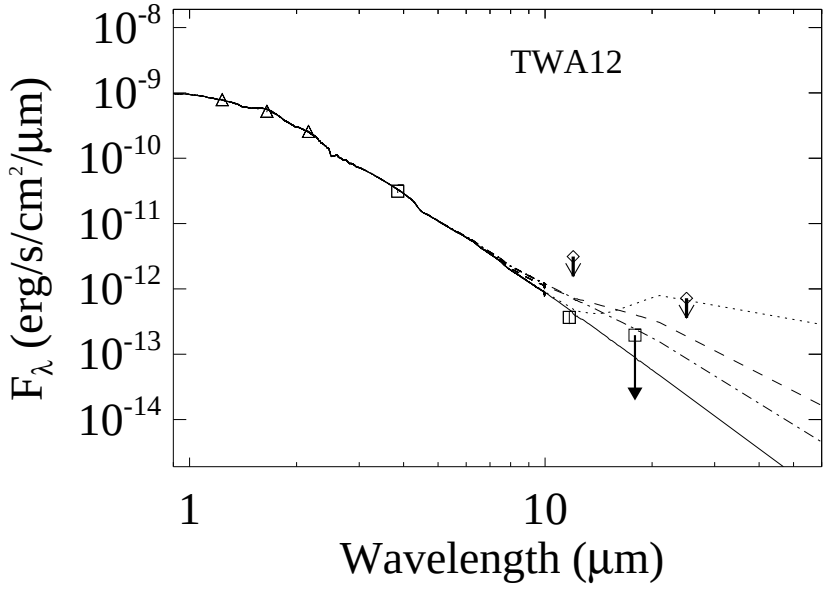

Fig. 2.— Spectral energy distribution of TWA 12 presented as an example of our excess limits. Triangles are J, H, and Ks data from 2MASS, squares are the LWS data reported in this paper, diamonds are the 150 mJy completeness level of IRAS at 12 μm and extrapolated to 18μm. The dotted, dashed, and dotted-dashed lines are the maximum 100 K, 200 K, and 300 K blackbodies of infrared excess that can be accommodated by our and the IRAS measurements at 3 σ.